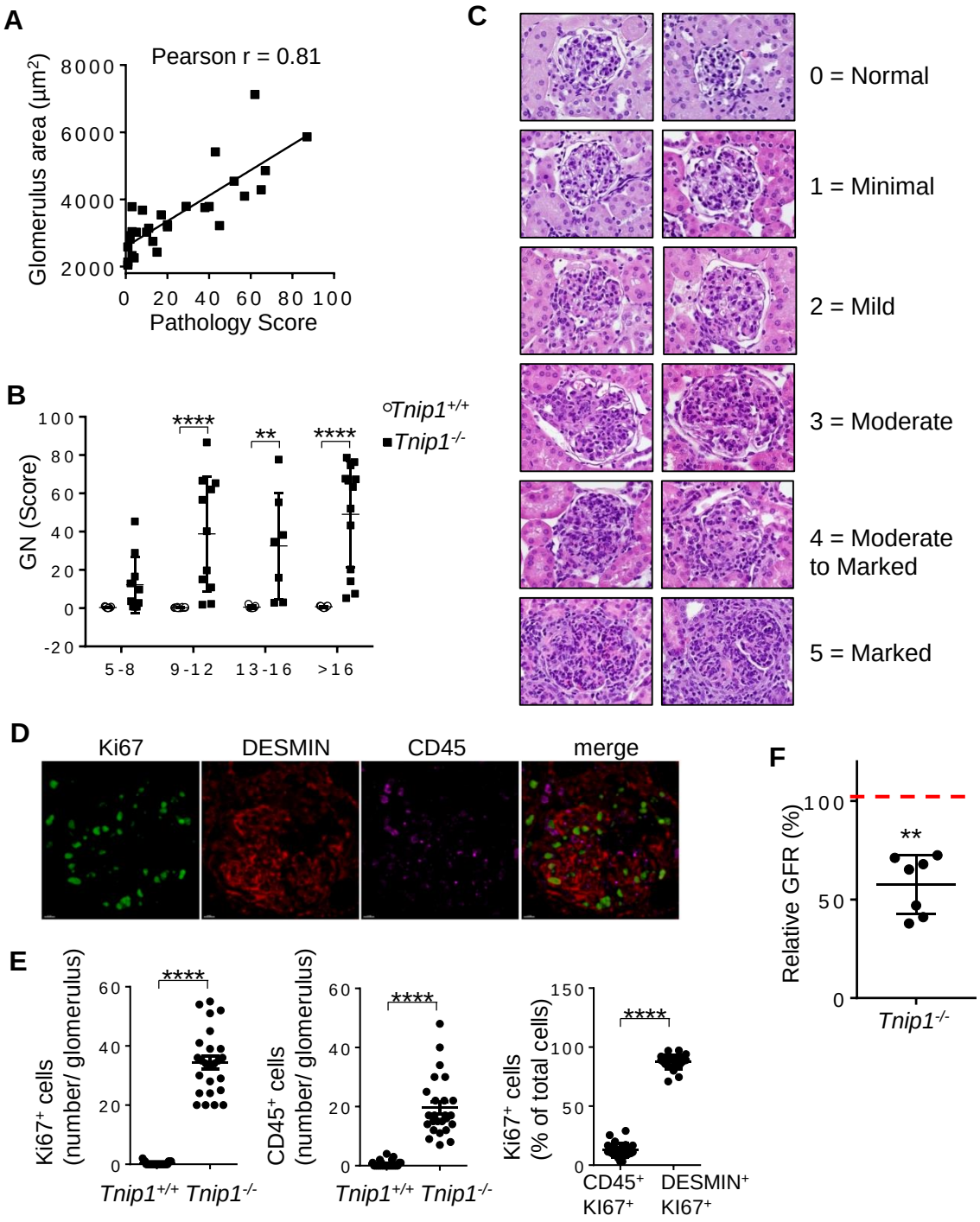

Figure S1. Glomerular pathology and glomerular filtration rate of *Tnip1*$^{-/-}$ *mice*
(**A**) Correlation of glomerular area and pathology score assessing GN in *Tnip1*$^{-/-}$ *mice.* Histology-based kidney pathology of *Tnip1*$^{-/-}$ *mice* (various age groups) was assessed by GN score and glomerular area measurements (detailed in Methods section), and is displayed as correlation analysis. Pearson r = Pearson correlation coefficient. (**B**) Kidney pathology as assessed by GN score of *Tnip1*$^{+/+}$ and *Tnip1*$^{-/-}$ *mice* during time. (**C**) H&E-stained kidney sections of *Tnip1*$^{-/-}$ *mice* showing examples of glomerular lesions with different grades used for scoring (see Methods section). Original magnification 400x.

Figure S1 (continued)
(**D**) Multicolor immunofluorescence analysis of kidney tissue sections from16 week-old *Tnip1*$^{-/-}$ *mice* using antibodies against Ki67, DESMIN and CD45. Scale bars 10 µm. (**E**) Quantitative analysis of multicolor immunofluorescence images (as shown in (E)) of 16 week-old *Tnip1*$^{+/+}$ and *Tnip1*$^{-/-}$ *mice.* (**F**) GFR of 20 week-old *Tnip1*$^{-/-}$ mice. GFR of *Tnip1*$^{+/+}$ littermates (n=7) served as control (100%). Data represent mean ± s.d.; *P < 0.05, **P < 0.01, ***P < 0.001; One-way Anova with Tukey's multiple comparison test (A); Mann-Whitney U test (C). Symbols represent data from individual mice.

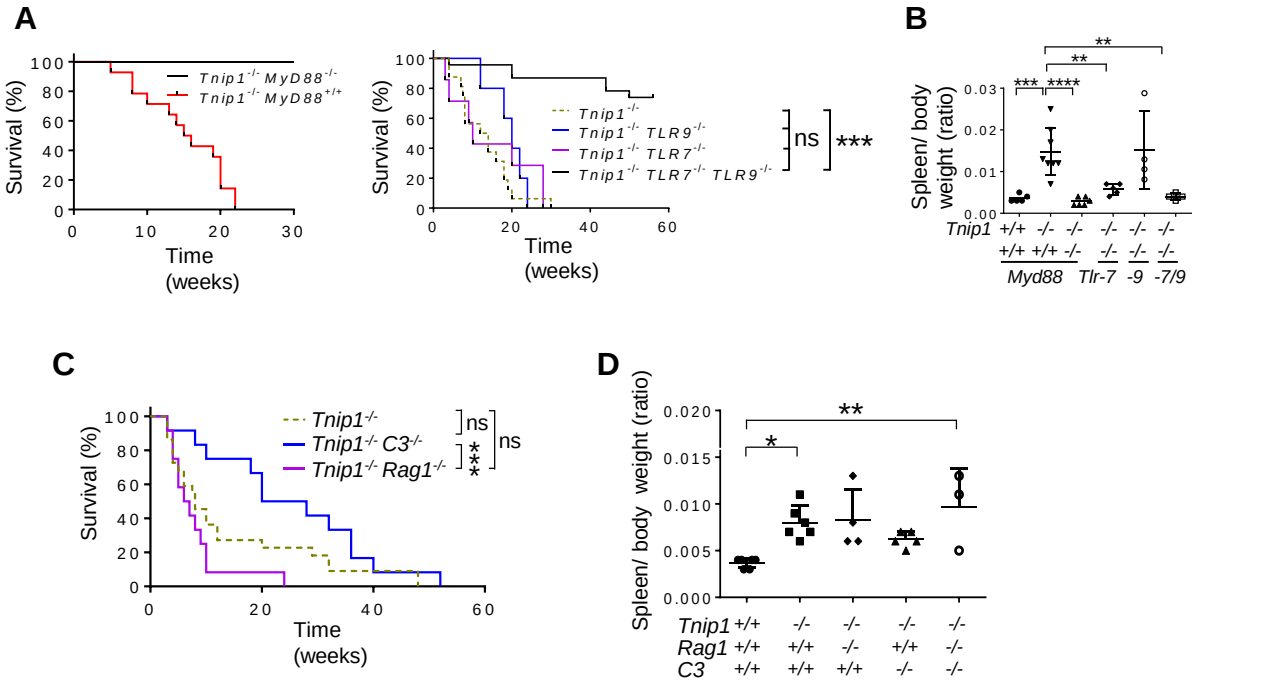

Figure S2. Survival and splenomegaly of *Tnip1*$^{-/-}$ *mice* with genetic deletion of TLR proteins, *Rag1* and *C3*

(**A**) Survival of mice with indicated genotype during time (*Tnip1*$^{-/-}$ *MyD88*$^{+/+}$, n=14; *Tnip1*$^{-/-}$ *MyD88*$^{-/-}$, n=18; *Tnip1*$^{-/-}$ *TLR9*$^{-/-}$, n=8, *Tnip1*$^{-/-}$ *TLR7*$^{-/-}$, n=7; *Tnip1*$^{-/-}$ *TLR9*$^{-/-}$ *TLR7*$^{-/-}$, n=23). (**B**) Spleen/ body weight ratio of 16 week-old mice with indicated genotype. (**C**) Survival of mice with indicated genotype during time (*Tnip1*$^{-/-}$, n=22; *Tnip1*$^{-/-}$ *C3*$^{-/-}$, n=12; *Tnip1*$^{-/-}$ *Rag1*$^{-/-}$, n=12). (**D**) Spleen/ body weight ratio of 12 week-old mice with indicated genotype. Data represent mean ± s.d. (B, D); *P < 0.05, **P < 0.01, ***P < 0.001; ****P < 0.0001. Mantel-Cox test (A, C); Anova with Tukey's multiple comparison test (B, D); Symbols represent data from individual mice.

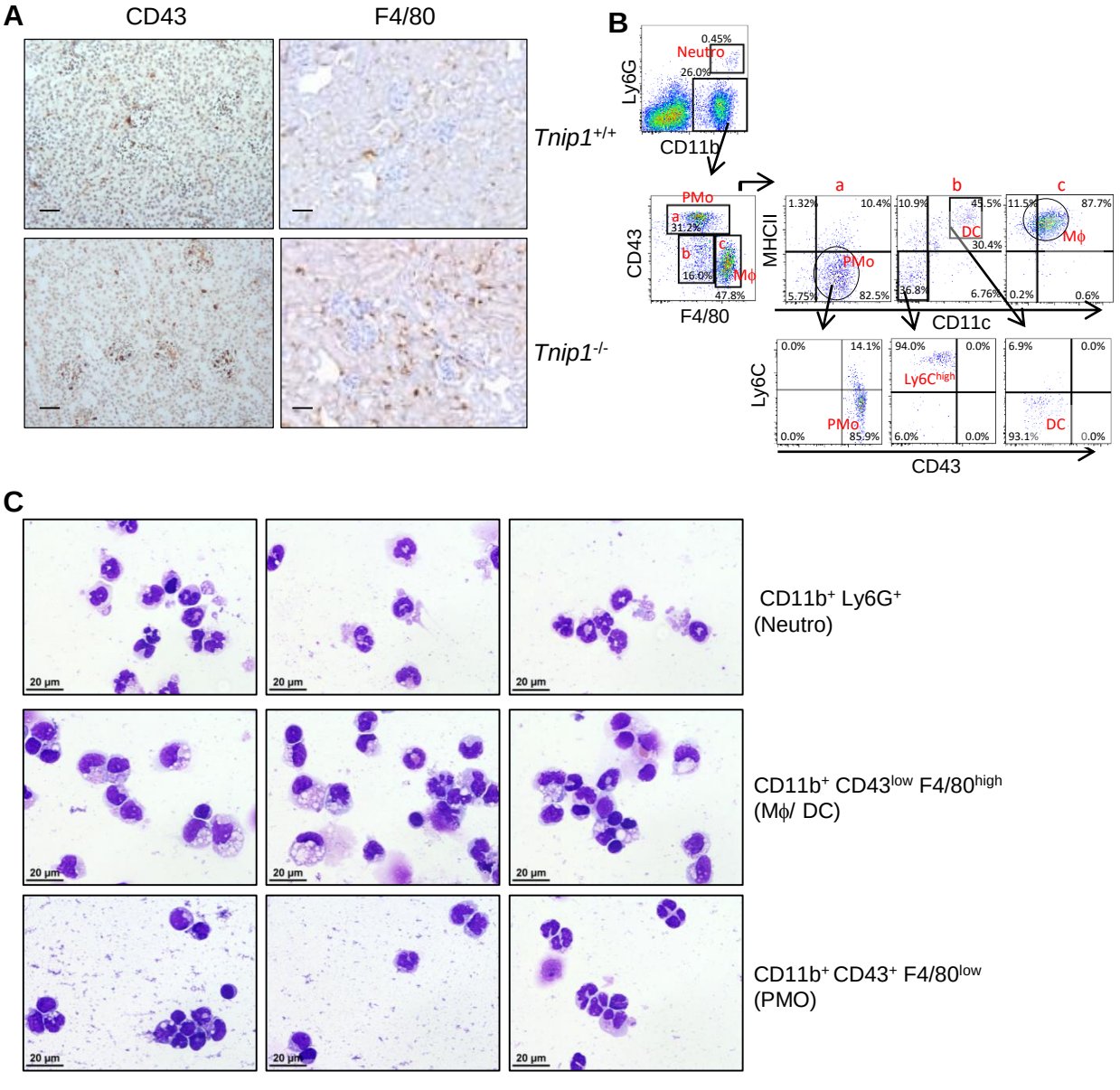

Figure S3. Characterization of immune cell populations in kidneys of *Tnip1*$^{-/-}$ mice
(**A**) Kidney histology (immuno-histochemistry) of 12-week-old *Tnip1*$^{+/+}$ and *Tnip1*$^{-/-}$ mice. (**B**) Flow cytometry and gating strategy of cells isolated from kidneys of *Tnip1*$^{-/-}$ mice. (**C**) May-Grünwald-stained cells that were isolated by flow cytometry-based cell sorting from immune cell populations depicted in Figure 4B. Scale bars 50 µm (A) and 20 µm (C).

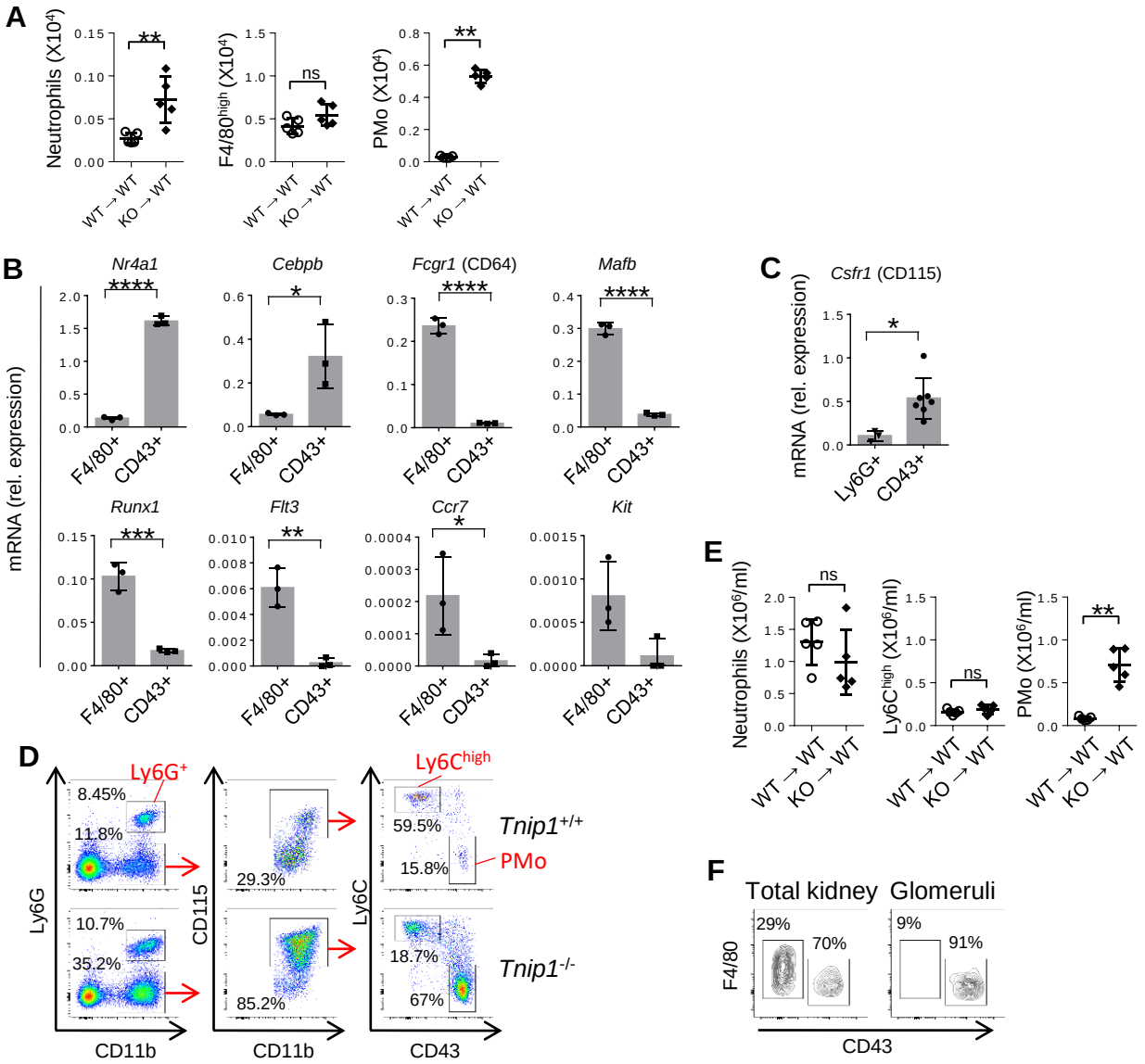

Figure S4. Characterization of PMo from kidneys, PB and BM chimeric mice

(**A**) Total numbers of indicated immune cell types isolated from kidneys of BM-chimeric *Tnip1*$^{+/+}$ recipient mice reconstituted with BM from *Tnip1*$^{+/+}$ (WT) or *Tnip1*$^{-/-}$ (KO) mice (12 weeks after transfer).(**B, C**) Q-PCR-analysis of FACS-sorted *Tnip1*$^{-/-}$ tissue macrophages (F4/80^{+}), PMo (CD43^{+}) and neutrophils (Ly6G^{+}) as defined in Figure S3B. Kidneys were obtained from chimeric mice based on BM from *Tnip1*$^{-/-}$ mice (25 weeks after BM transfer). (**D**) Flow cytometry-based gating strategy of PMo from the PB of *Tnip1*$^{+/+}$ and *Tnip1*$^{-/-}$ mice. (**E**) Total numbers of indicated immune cell types isolated from the PB of BM chimeric mice described in (A). (**F**) Flow cytometry analysis of cells isolated from total kidneys (left) and purified glomeruli (right) of 25 week-old *Tnip1*$^{-/-}$ mice. Symbols represent data from individual mice. Data represent mean ± s.d.; *P < 0.05, **P < 0.01, ***P < 0.001; ****P < 0.0001; unpaired t test (B-C); Mann-Whitney U test (A, E).

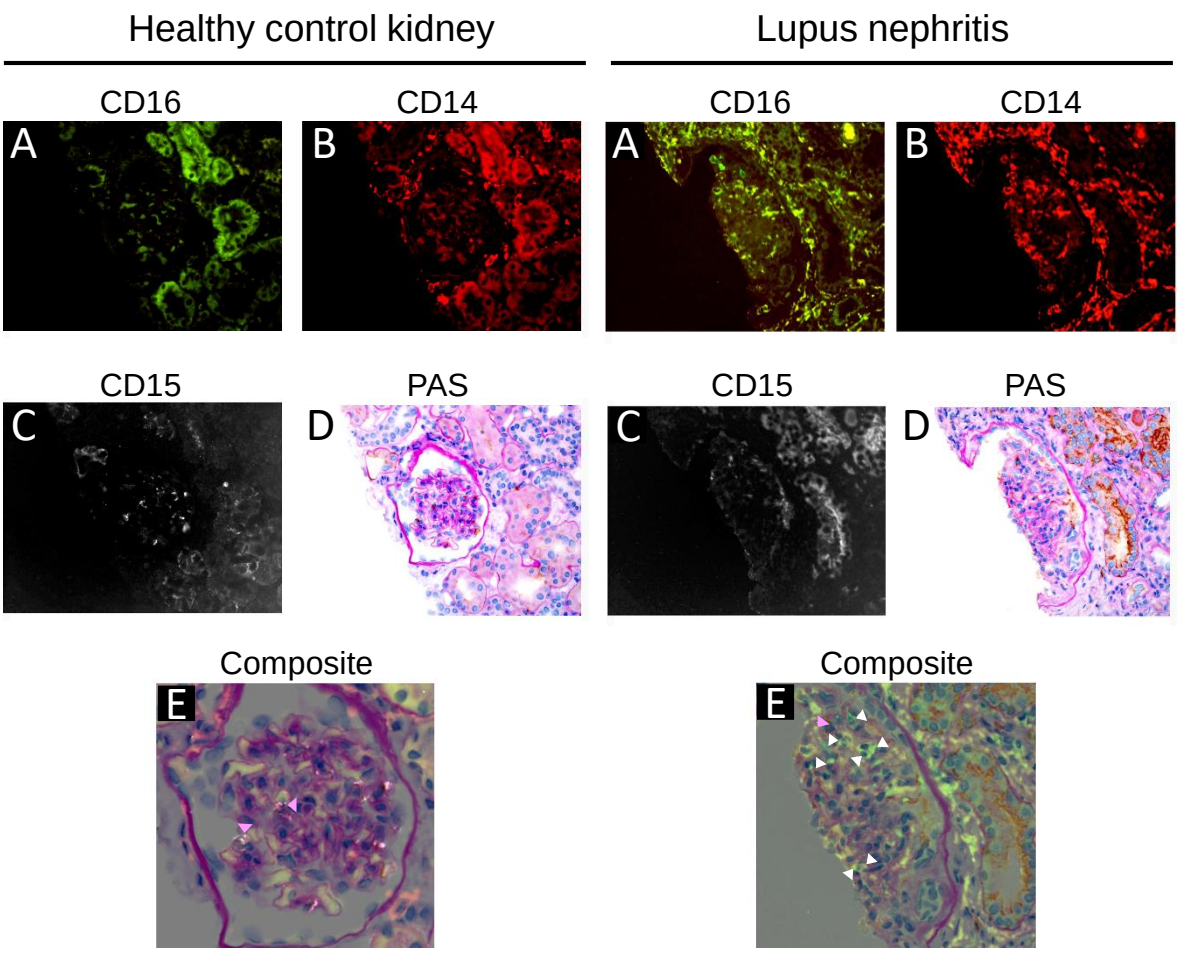

Figure S5. Image analysis of patrolling monocytes in human lupus nephritis
Photo montage of glomeruli from a control patient with a reperfusion renal transplant biopsy (left side) and a patient with lupus nephritis (Class IV-G, right side). CD16 (**A**); CD14 (**B**); CD15 (**C**); Periodic-acid Schiff reaction (PAS)(**D**); Composite of all stains with $CD16^{+}$ $CD14^{-/dim}$ $CD15^{-}$ cells indicated with white arrow heads and $CD15^{+}$ cells indicated with magenta arrowheads (**E**). Original magnification 400x.

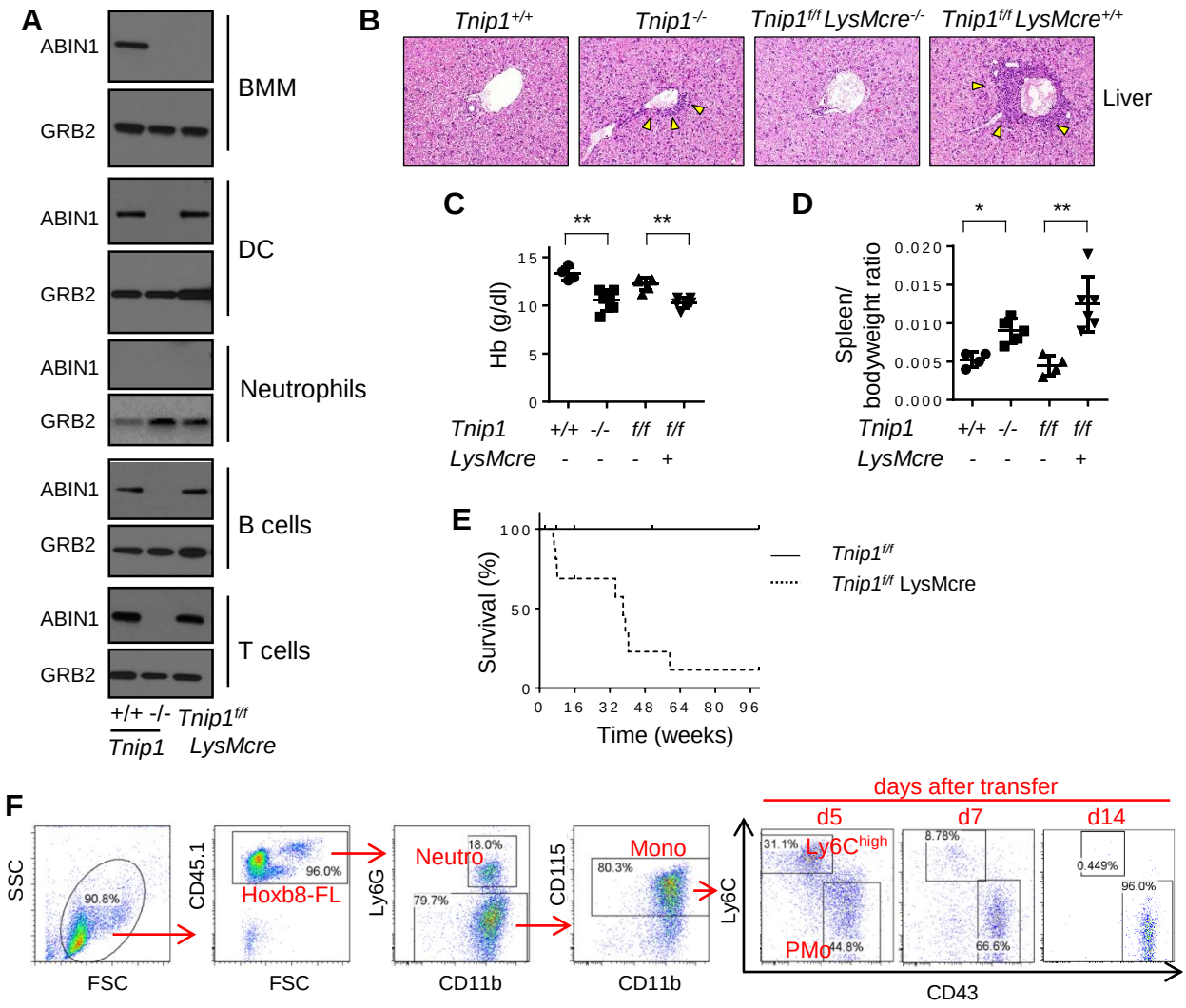

Figure S6. Cell type-specific deletion of ABIN1 in *Tnip1*$^{f/f}$ LysMcre mice and time course of Hoxb8-FL-derived monocyte differentiation in the PB of adoptively transferred mice

(**A**) Immuno-blot analysis of ABIN1 expression of indicated immune cell types from 12 week-old mice that were isolated based on flow cytometry-activated cell sorting (FACS) from BM (neutrophils) and spleen (T-cells, B-cells), or that were in vitro generated using BM and L-cell-conditioned medium (BMM) or GM-CSF (DC). Cells were sorted as CD11b^{+} Ly6G^{+} neutrophils, CD11b^{-} CD3^{+} T-cells and CD11b^{-} CD19^{+} B-cells. (**B**) Liver pathology of 16 week-old mice assessed by H&E-staining. Representative images are shown. (**C,D**) Anemia and splenomegaly in *Tnip1*$^{fl/f}$ LysMcre mice assessed by analysis of spleen and body weight of 12-16 week-old mice (depicted as ratio of spleen/ body weight)(C) and analysis of hemoglobin concentration in the peripheral blood (**E**). Survival of *Tnip1*$^{f/f}$ and *Tnip1*$^{f/f}$ LysMcre mice during time. (**F**) Flow cytometry analysis of PB from lethally irradiated mice that were adoptively transferred with non-differentiated Hoxb8-FL cells. PB was analyzed 5, 7 and 14 days after Hoxb8-FL cell transfer. The upper panel shows the gating strategy for monocytes, the lower panel shows the time course of Ly6C^{high} (classical) and PMo (Ly6C^{low} non-classical) monocytes in the PB.

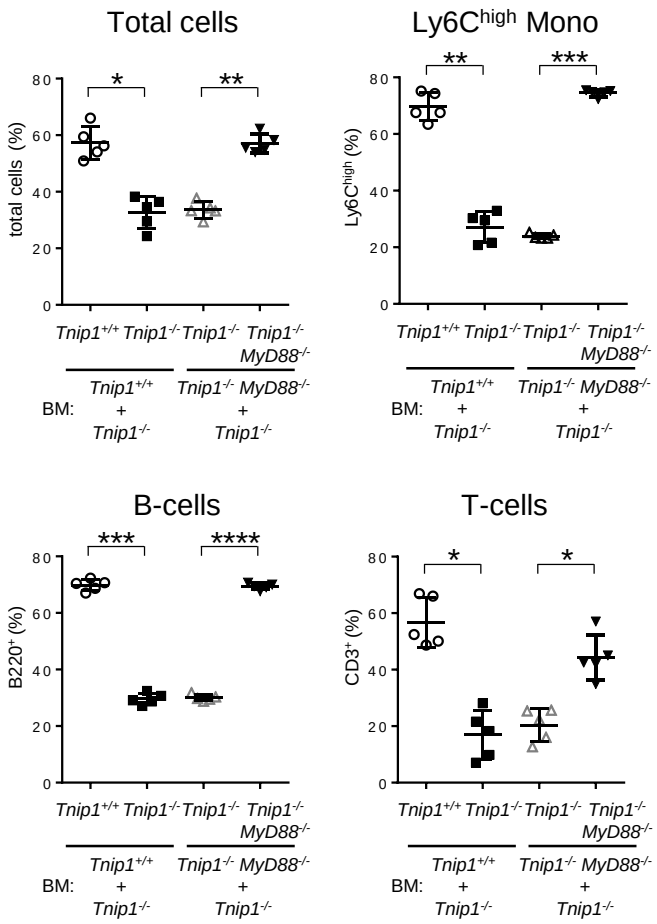

Figure S7. ABIN1 controls cell-intrinsically MyD88-mediated PMo deregulation
Cell numbers of total white blood cells (WBC), Ly6C^{high} monocytes, B220^{+} B-cells and CD3^{+} T-cells in the PB blood of BM chimeras (6 weeks after transfer) which were established with BM from *Tnip1*$^{+/+}$ and *Tnip1*$^{-/-}$ mice, or from BM from *Tnip1*$^{-/-}$ and *Tnip1*$^{-/-}$ *Myd88*$^{-/-}$ mice. Relative cell numbers derived from *Tnip1*$^{+/+}$ vs. *Tnip1*$^{-/-}$ BM and *Tnip1*$^{-/-}$ vs.*Tnip1*$^{-/-}$ *Myd88*$^{-/-}$ BM are shown.
Data represent mean ± s.d.; *P < 0.05, **P < 0.01, Mann-Whitney U test. Symbols represent data from individual mice.

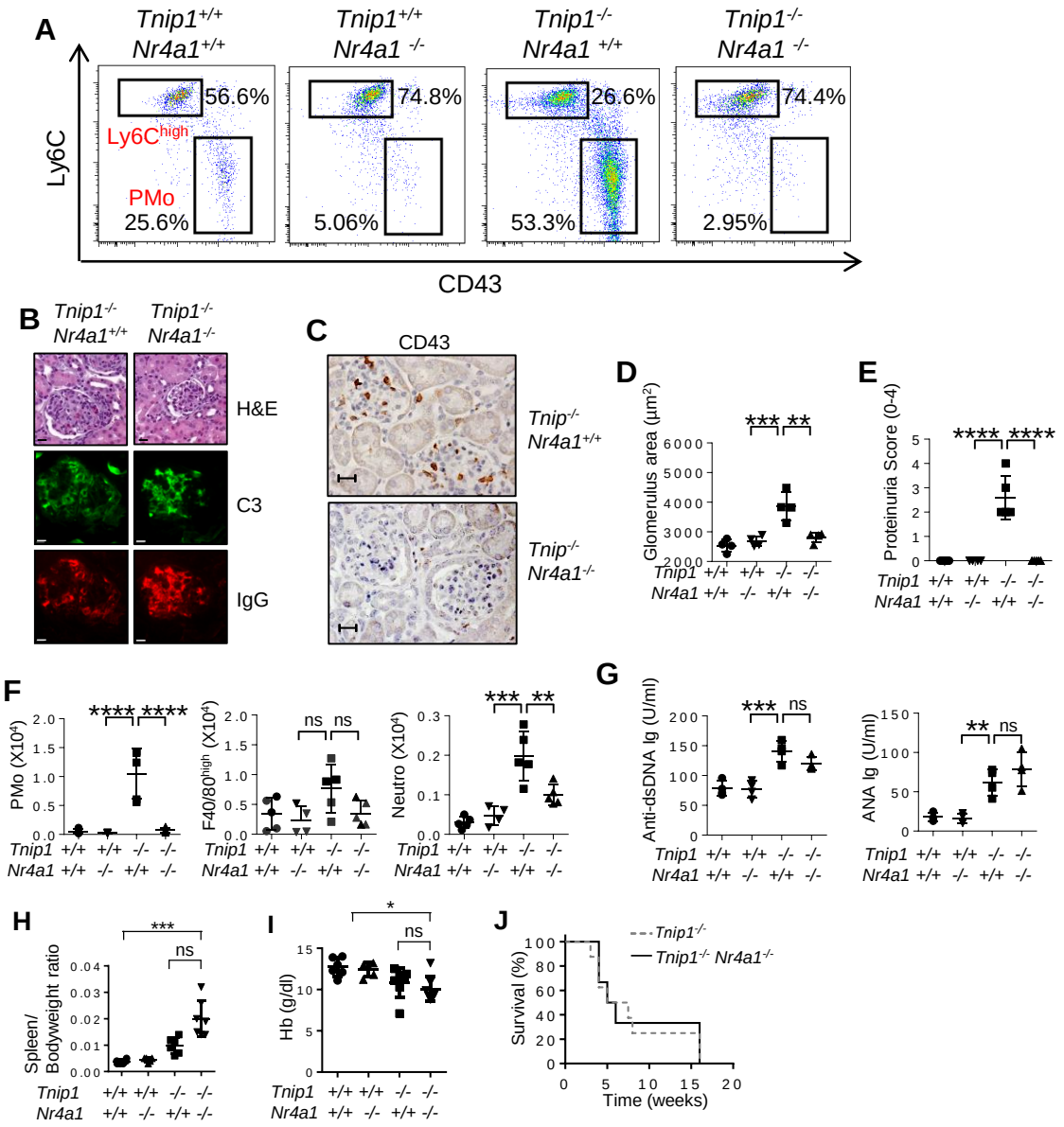

Figure S8. Genetic suppression of PMo protects from GN

(**A**) Flow cytometry analysis of PB from 12-week-old mice with indicated genotype. CD11b^{+} Ly6G^{-} CD115^{+} monocytes are shown. (**B-E**) Kidney pathology and function of 16-week-old *Tnip1*$^{-/-}$ and *Tnip1*$^{-/-}$ *Nr4a1*$^{-/-}$ mice as analyzed by histology based on H&E-staining and antibodies against C3 and IgG (**B**), CD43 (**C**), the measurement of avg. glomerulus size (**D**) and protein concentration in urine (**E**). Representative glomeruli are shown. (**F**) Total numbers of CD43^{+} PMo, F4/80^{high} myeloid cells and Ly6G^{+} neutrophils isolated from the kidneys of 16-old *Tnip1*$^{-/-}$ and *Tnip1*$^{-/-}$ *Nr4a1*$^{-/-}$ mice. (**G**) Serum levels of anti-dsDNA Ig and ANA of 16-week-old *Tnip1*$^{-/-}$ and *Tnip1*$^{-/-}$ *Nr4a1*$^{-/-}$ mice. (**H,I**) Anemia and splenomegaly in *Tnip1*$^{-/-}$ and *Tnip1*$^{-/-}$ *Nr4a1*$^{-/-}$ mice assessed by analysis of spleen and body weight of 16 week-old mice (depicted as ratio of spleen/ body weight)(H) and analysis of hemoglobin concentration in the peripheral blood (G). (**J**) Survival of *Tnip1*$^{-/-}$ and *Tnip1*$^{-/-}$ *Nr4a1*$^{-/-}$ mice during time. Scale bars 20 µm. Data represent mean ± s.d.; *P < 0.05, **P < 0.01; One-way Anova with Tukey's multiple comparison test (D-I). Symbols represent data from individual mice. Ns=not significant.